Three-dimensional Patterns and Redistribution of Myosin II and Actin in Mitotic *Dictyostelium* Cells

Ralph Neujahr, Christina Heizer, Richard Albrecht, Maria Ecke, Jean-Marc Schwartz, Igor Weber, and Günther Gerisch

Max-Planck-Institut für Biochemie, D-82152 Martinsried, Germany

Abstract. Myosin II is not essential for cytokinesis in cells of *Dictyostelium discoideum* that are anchored on a substrate (Neujahr, R., C. Heizer, and G. Gerisch. 1997. *J. Cell Sci.* 110:123–137), in contrast to its importance for cell division in suspension (DeLozanne, A., and J.A. Spudich. 1987. *Science.* 236:1086–1091; Knecht, D.A., and W.F. Loomis. 1987. *Science.* 236: 1081–1085.). These differences have prompted us to investigate the three-dimensional distribution of myosin II in cells dividing under one of three conditions: (*a*) in shaken suspension, (*b*) in a fluid layer on a solid substrate surface, and (*c*) under mechanical stress applied by compressing the cells. Under the first and second conditions outlined above, myosin II does not form patterns that suggest a contractile ring is established in the furrow. Most of the myosin II is concentrated in the regions that flank the furrow on both sides towards the poles of the dividing cell. It is only when cells are compressed that myosin II extensively accumulates in the cleavage furrow, as has been previously described (Fukui, Y., T.J. Lynch, H. Brzeska, and E.D. Korn. 1989. *Nature.* 341:328–331), i.e., this massive accumulation is a response to the mechanical stress. Evidence is provided that the stress-associated translocation of myosin II to the cell cortex is a result of the dephosphorylation of its heavy chains. F-actin is localized in the dividing cells in a distinctly different pattern from that of myosin II. The F-actin is shown to accumulate primarily in protrusions at the two poles that ultimately form the leading edges of the daughter cells. This distribution changes dynamically as visualized in living cells with a green fluorescent protein–actin fusion.

Mitotic cell division involves the formation of a cleavage furrow, typically induced in the middle of a cell precisely after segregation of the chromosomes along the spindle. The furrow is a constriction of the cell body brought about by local differences in the activity or in the distribution of proteins associated with the actin-rich cortex of the cells. Actin and myosin are thought to play a prominent role in formation of the furrow. Filaments of actin and myosin II have been proposed to form, at the final stage of mitosis, an equatorial ring that separates the daughter cells by active contraction (Opas and Soltynska, 1978; Maupin and Pollard, 1986; Yonemura and Kinoshita, 1986; Cao and Wang, 1990*a*,*b*; Otto and Schroeder, 1990; Schroeder, 1990; Satterwhite and Pollard, 1992; Mabuchi, 1994). Nevertheless, the particular pattern formed by actin filaments in the cleavage furrow and the infrequent accumulation of myosin II in that region have questioned the significance of a ring formed by appropriately oriented actin and myosin filaments as the sole basis of mitotic cleavage in an animal cell (Nunnally et al., 1980; Fishkind and Wang, 1995).

Support for the contractile ring concept has been provided in *Dictyostelium* by the observation that the conventional, double-headed myosin II strongly accumulates in the region of the furrow (Yumura et al., 1984; Fukui et al., 1989; Kitanishi-Yumura and Fukui, 1989) and in the same region actin filaments form arrays pointing into different directions (Fukui and Inoué, 1991). In these studies on dividing *Dictyostelium* cells, extensive accumulation of myosin II in the cleavage furrow has been shown using cells compressed by physical sandwiching between a glass and agar surface (Yumura et al., 1984). In interphase cells, this compression is known to result in the recruitment of myosin II from the cytoplasm to the border of the cells, where it assembles in a crescent-like fashion (Gerisch et al., 1993). Here we show that in mitotic cells, the mechanical stress-induced translocation of myosin II leads first to its redistribution to the cell cortex and second to its almost quantitative transport to the cleavage furrow. Based on the results presented herein, changes in the organization of myosin II and actin that are intrinsic to cytokinesis can be distinguished from supplementary ones that vary with the conditions under which the cells divide. This distinc-

Address all correspondence to Günther Gerisch, Max-Planck-Institut für Biochemie, D-82152 Martinsried, Germany. Tel.: (49) 89-8578-2326. Fax: (49) 89-8578-3885. E-mail: gerisch@biochem.mpg.de

tion is relevant in the light of recent findings indicating that myosin II stabilizes a cleavage furrow in *Dictyostelium* cells but is not essential for its formation provided that the cells adhere to a solid substrate surface (Neujahr et al., 1997).

Materials and Methods

Culture Conditions for Analyzing Cytokinesis

Dictyostelium discoideum wild-type strain AX2-214, the GFP–α-tubulin–expressing transformant HG1668, and the triple-ala mutant HG1555 (Lück-Vielmetter, 1992) were cultivated in nutrient medium at 21–23°C to a density of not more than 5 x 10^6 cells per ml. HG1668 produces a fusion of α-tubulin from *D. discoideum* with green fluorescent protein (GFP)[1] at its NH_2 terminus. The vector was constructed in a similar way as described for GFP–actin (Westphal et al., 1997). In the triple-ala mutant, the three phosphorylatable residues Thr1823, Thr1833, and Thr2029 at the myosin II heavy chains are converted into alanine (Lück-Vielmetter et al., 1990). The GFP–actin–expressing transformant HG1662 (Westphal et al., 1997) and the GFP-myosin II heavy chain–expressing transformant of the myosin II–null strain HS1 (Moores et al., 1996) were cultivated in nutrient medium in plastic petri dishes. To increase the mitotic index, the cells were synchronized as described by Neujahr et al. (1997). In the reflection interference contrast microscopy (RICM) studies, cells were cultivated on SM agar plates with *Klebsiella aerogenes* (Sussman, 1966).

In immunolabeling studies of different stages of cytokinesis, cells were cultivated in nutrient medium in suspension on a rotary shaker at 150 rpm or attached to a glass surface. For in vivo microscopy, cells attached to glass were incubated with a suspension of *Klebsiella aerogenes* in 17 mM K/Na-phosphate buffer, pH 6.0 (non–nutrient buffer). The agar overlay method of Yumura et al. (1984) was used to compress cells. The cells adhering to a glass surface were covered by 0.2-mm-thick pieces of 2% ME agarose (SEAKEM; FMC BioProducts, Rockland, ME). Excess fluid was removed by soaking with filter paper under microscopic control. The time point t_0 for myosin II redistribution represents the moment when this step was completed and the cells were extensively flattened.

Immunofluorescence Microscopy and Scanning Electron Microscopy of Fixed Cells

For indirect immunofluorescence labeling, surface-attached cells were fixed with picric acid/paraformaldehyde for 20 min at room temperature and postfixed with 70% ethanol as described by Humbel and Biegelmann (1992). Cells dividing in shaken culture were fixed directly from the suspension by the same volume of double-concentrated picric acid/paraformaldehyde solution, and all the following steps were performed in suspension, with centrifugation steps between, before finally attaching the labeled cells to a poly-L-lysine–coated coverslip and embedding them in mounting medium (Jungbluth et al., 1994). For comparison, cells attached to a glass surface were fixed in 1% formaldehyde in acetone according to Egelhoff et al. (1991) for 5 min at −15°C. The primary antibodies used were mouse anti–myosin II mAb 56-396-5, which recognizes both monomeric and filamentous myosin II (Pagh and Gerisch, 1986), and rat anti–α-tubulin mAb YL-1/2 (Kilmartin et al., 1982) purchased from Dunn Labortechnik (53567; Asbach, Germany). Secondary antibodies for confocal imaging were Cy3-conjugated goat anti–mouse IgG (Jackson ImmunoResearch, West Grove, PA) or FITC-conjugated goat anti–rat IgG (Sigma Chemical Co., St. Louis, MO). For conventional fluorescence microscopy, TRITC-conjugated goat anti–mouse IgG (Jackson ImmunoResearch) was used. TRITC-conjugated phalloidin (Sigma Chemical Co.) was applied to label F-actin for Fig. 8.

For conventional fluorescence microscopy, a microscope (model Axiophot; Carl Zeiss, Jena, Germany) with a 100×/1.3 Plan-NEOFLUAR objective was used, and micrographs were taken on Fuji Neopan 400 ASA film (Tokyo, Japan). Confocal microscopy was performed on a Zeiss LSM 410 using a 63×/1.4 Planapochromat or a 40×/1.3 NEOFLUAR for Cy3, TRITC, and FITC fluorescence images and a 100×/1.3 Plan-NEOLUAR for GFP images. For three-dimensional image reconstruction, confocal sections were scanned at distances of 0.2 μm in the z-axis with pixel sizes of 50 nm in the x- and y-axes. The full width at half maximum of the point spread function was calculated under the conditions used for myosin immunofluorescence imaging as 0.24 μm in the x- and y-axes and 0.57 in the z-axis.

For scanning electron microscopy, cells dividing in nutrient medium were fixed with 0.2% osmic acid and 2% glutaraldehyde (Claviez et al., 1986), and micrographs were obtained using a microscope (model SM 35C; JEOL U.S.A., Inc., Peabody, MA) with Ilford PanF 50 ASA film. Photographic images were digitized for printing using a Scan Jet IIcx (Hewlett-Packard, Palo Alto, CA).

Three-dimensional Image Construction and Color Coding

Confocal images were processed using the AVS program (Advanced Visual Systems, Waltham, MA), running on a DEC-alpha (Digital Corporation, Maynard, MA). The digitized fluorescence images from the confocal microscope formed a three-dimensional data set, containing gray levels of voxels between 0 and 255. This data set representing the continuous spatial distribution of emitted light intensities was used to calculate the cellular distribution of fluorescent antibody or phalloidin. Voxel size in the z direction was adjusted to that in the x and y directions by linearly interpolating three additional planes.

The gray levels were used as an index to a color map. They were converted to a color data set in the hue-saturation-brightness color coordinate system. For each reconstruction, we provide a color bar representing a linear scale of gray values converted into a color code. The background value is indicated on the left-hand side of each bar. At least 98% of the voxels are within the range of gray values indicated on the right-hand side of each bar. Any voxel with a higher gray value is assigned the same red color.

The next step in image construction was a conventional ray tracing process (Levoy, 1988). For each pixel in the final image plane, a ray is cast into the volume. The color map has an additional entry, the transparency value α, required for constructing the three-dimensional image. The ray represents a path of integration in the viewing direction over the α values. Each voxel passed by the ray contributes to the final color, which is projected to the image plane. Integration along a ray is performed until a prescribed α value of 1.0 is reached. The α values are summed, and the color values are averaged along the casting ray. This averaging decreases the saturation of colors. Adjusting the hue, saturation, brightness, transparency, and the projection angle of the casting rays led to the final three-dimensional reconstructions.

In the presented three-dimensional images, α values below a threshold that corresponds to the amplitude of background outside the cells were set to zero so that these areas appear black in the images. α values above threshold were set to 1/9. As a result, beginning with the first voxel above background, about 500 nm in the viewing direction (including the unsharp portion described by the point spread function) contributed to the final surface color. This means the fluorescence intensities of inner regions of a cell are hidden. Because of the digitalization and ray-tracing procedure, the color of the cell borders hit by the casting rays at low angle is shifted towards lower values in the color map as compared with the regions that are hit orthogonally. For example, the color of the upper surfaces in the cells shown in Fig. 1 is shifted towards blue.

To represent the measured fluorescence intensities in the inner regions of a cell, the three-dimensional data set was sectioned along different planes. Colors in these planes correspond to the fluorescence intensities indicated by the color bars in the figures. To interpret the cross sections presented in panels 8 of Figs. 3, 4, 7, and 8, the asymmetry of the point spread function in z- versus x- and y-axes should be taken into account. For an assumed fluorescent layer of 300-nm thickness and intensity of 1.00, calculation yields a reduction in apparent fluorescence intensities to 0.52 in the z direction and 0.95 in the x or y directions.

In Vivo RICM and Fluorescence Microscopy

For recording cell shape, substrate adhesion, and GFP fusion proteins in the course of cytokinesis, cells were placed in an open chamber on a glass coverslip on the stage of an inverted microscope. The cells divided in non–nutrient buffer supplemented with *Klebsiella aerogenes*. This buffer was used to circumvent the presence of fluorescent compounds in the nutrient medium that can sensitize the cells to light (Westphal et al., 1997).

A double-view microscope was used for simultaneous phase-contrast microscopy and RICM as described by Weber et al. (1995). Cells adhering

1. *Abbreviations used in this paper*: GFP, green fluorescent protein; RICM, reflection interference contrast microscopy.

to a glass surface coated with BSA were observed with an inverse microscope (model Axiovert 135; Carl Zeiss) equipped with an ANTIFLEX-NEOFLUAR, 63×/1.25 objective. For confocal recording of GFP fluorescences, cells dividing under an agar overlay were imaged using a Zeiss LSM 410 equipped with a 100×/1.3 Plan-NEOFLUAR.

Results

Shape Changes and Myosin II Distribution in Dictyostelium Cells Dividing in Suspension

To determine the shape of wild-type cells dividing in suspension and to localize myosin II in the cortical region, cells from a shaken culture were fixed and double-labeled with antibodies against α-tubulin and myosin II. The α-tubulin label was used to identify cells in mitotic and early post-mitotic stages. In Fig. 1, five examples are shown in a sequential order. The data indicate that cells become elongated at telophase, and furrowing proceeds during post-telophase essentially in a rotationally symmetrical fashion. Protrusions are localized to the polar regions of the suspended cells (Fig. 1 *D*), similar to the protrusions actively extended and retracted by cells dividing on a glass surface, which are rich in F-actin and coronin (Neujahr et al., 1997).

The actin-rich cortex of *Dictyostelium* cells is 100–200 nm thick (Hanakam et al., 1996), in accord with its thickness in other cells (Schroeder, 1990). To illustrate the distribution of myosin II close to the cell surface, fluorescence intensities collected from confocal sections were used for a three-dimensional representation. The myosin proved to be moderately enriched in the regions on both sides of the cleavage furrow (Fig. 1, *left*). No sharply outlined enrichment of myosin II in the furrow was seen in cells that divided in suspension—that is under conditions where myosin II is required for cleavage (DeLozanne and Spudich, 1987; Knecht and Loomis, 1987).

Substrate Contact During Cytokinesis on a Solid Surface

Shape changes in cells dividing on a solid substrate were similar to those in suspension, with the exception that the cleavage furrow originated exclusively from the top and lateral surfaces of the cells (Fig. 2 *A*). Large areas on the bottom surface of the cells remained in contact with the substrate until the final stages of cytokinesis (Fig. 2 *B*). These areas included the tips of filopods and other surface extensions at the poles of the dividing cells, and also the entire length of the cleavage furrow. The furrow lost contact with the substrate when only a thin thread of cytoplasm spanned the gap between the daughter cells. This thread was stretched out within the fluid medium and was finally disrupted when the cells moved apart.

Although the support provided by a solid substrate enables mutant cells of *D. discoideum* to form a cleavage furrow and to complete cytokinesis in the absence of myosin II, its presence speeds up cytokinesis and improves the reliability of cleavage (Neujahr et al., 1997). To provide a basis

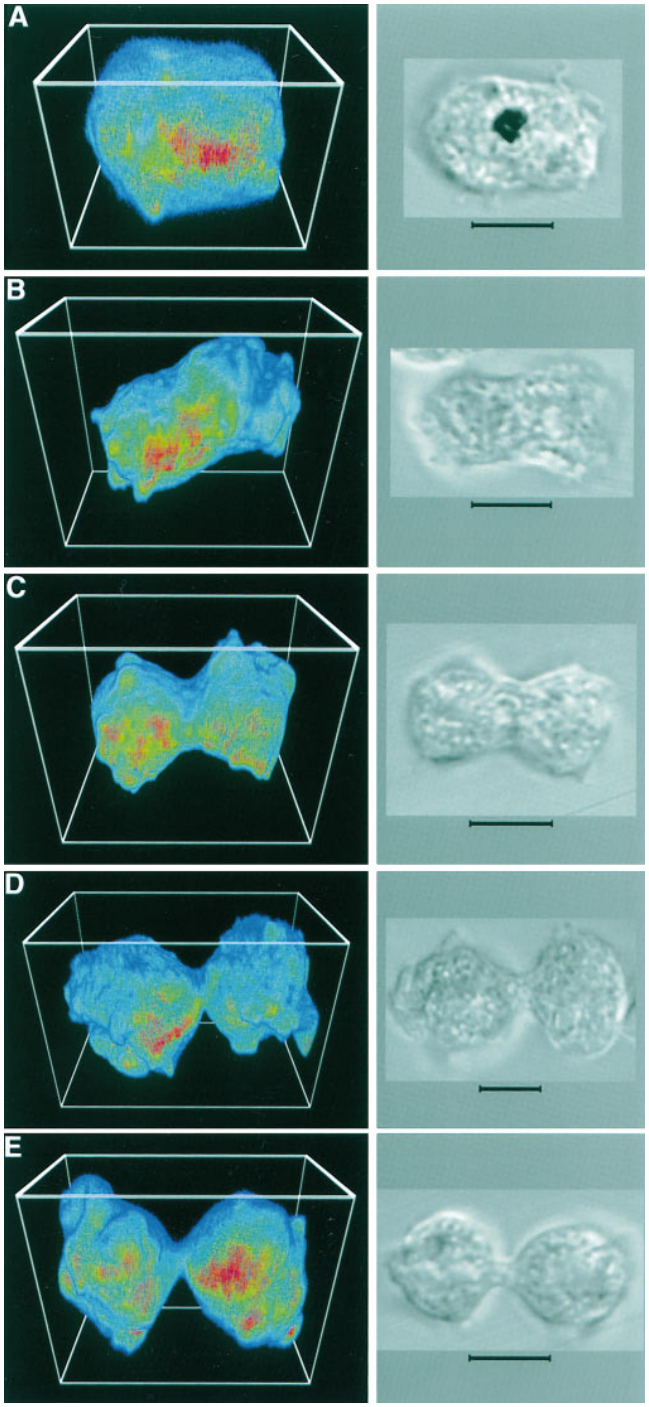

Figure 1. Stages of cytokinesis (*A–E*) in suspended cells of *Dictyostelium discoideum*. Cells growing in shaken suspension with liquid medium were fixed and labeled with antibodies for myosin II and α-tubulin. Mitotic cleavage stages identified by their microtubule organization were subjected to confocal imaging. (*Left*) Three-dimensional reconstructions based on the immunolabel of myosin II. Since myosin II is distributed within the entire cytoplasmic space, it could be used to visualize the shape of the dividing cells. Low to high concentrations of myosin II in the cell cortex are color-coded from dark blue to red. It should be noted that the ray tracing technique used reflects primarily the distribution of myosin II in those cortical regions of the cells that are faced towards the observer. In other regions of the three-dimensional images, the colors are shifted towards blue. For details of the imaging technique applied we refer to Materials and Methods. (*Right*) Cell shape as revealed by differential interference contrast microscopy. The dark spot in *A* is most likely an engulfed contaminating particle. What appears as an extension on the right in *D* is in fact another cell close to the dividing one. Bars, 10 μm.

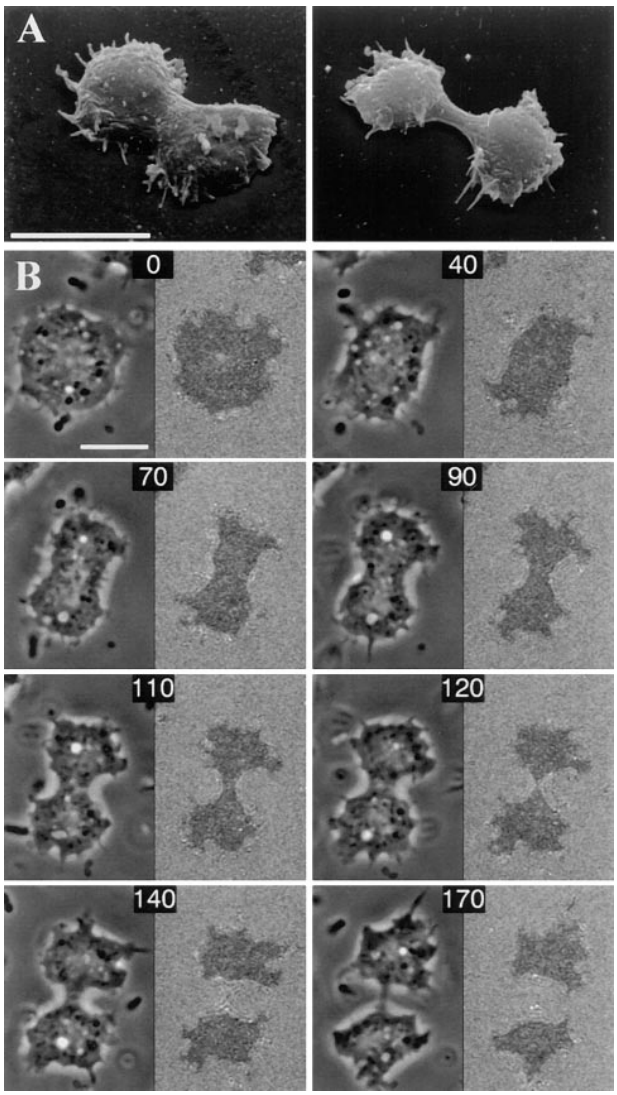

Figure 2. Shape changes of substrate attached *D. discoideum* cells. (*A*) Scanning electron micrographs of an early (*left*) and late (*right*) cleavage stage. Formation of the cleavage furrow from the top and lateral surfaces of the cells is recognizable as well as anchorage of the cells on the substrate by extensions of their polar regions. (*B*) Pairs of phase-contrast (*left*) and RICM images (*right*) of a cell undergoing cytokinesis. The numbers are seconds required for the cell to proceed from a rounded state to the end of cleavage. The transit from initiation of the furrow (between 40 and 70 s) to the final stage of cleavage takes only 2 min. The dark areas in the RICM images indicate that the cell has been in contact with the substrate not only with the extensions at its poles, but over most of its basal surface including the furrow region. Interference fringes at the 140- and 170-s stages indicate the detachment from the substrate of a strand that still connects the daughter cells. Bars, 10 μm.

for the interpretation of these effects, we analyzed the location of myosin II in wild-type cells anchored to a substrate.

Three-dimensional Myosin II Patterns in Early and Late Stages of Cytokinesis on a Substrate Surface

Figs. 3 and 4 illustrate the distribution of myosin II in consecutive stages of cell division on a glass surface. For each of the four cells shown in these figures, data are compiled in the following way. Panel *1*'s depict microtubule organization to confirm that the respective cell was in telophase (Fig. 3) or post-telophase (Fig. 4). Panels *2–5* show the myosin II label in four confocal sections through the cell from a plane close to the substrate to a plane close to the free upper surface of the cell. These panels illustrate the data on which three-dimensional image reconstructions are based. Panels *6–9* represent color-coded image constructions based on serial confocal sections. Panel *6*'s show a three-dimensional view of the particular cell analyzed, in which the distribution of myosin II beneath the cell surface is represented, comparable to that shown for the suspended cells in Fig. 1. Panels *7–9* show optically opened cells. The cells were either unroofed to view their bottom half (*7*), cross sectioned through the cleavage furrow (*8*), or vertically sectioned along their midline (*9*). Red color has been attributed to the highest intensity of myosin II antibody labeling.

At the earliest stage of cleavage, shown in Fig. 3 *A*, myosin II accumulated in the cortical region of the cell in the form of a diffuse zone along the midregion of the cell (Fig. 3, A_2–A_7). Optical cross sectioning revealed that the myosin II did not accumulate in a closed ring but was concentrated primarily in an asymmetrical fashion at both sides of the furrow (Fig. 3 A_8). Accordingly, no prominent accumulation of myosin II was recognized in the midline section of the cell (Fig. 3 A_9). At a more advanced cleavage stage, shown in Fig. 3 *B*, myosin II was similarly distributed as in the earlier stage. The myosin II enriched zone in the cell cortex was more prominent (Fig. 3 B_7). In this particular case, the myosin II pattern in the cross section almost formed a continuous ring. However, according to the image of the midline section, the myosin II was remarkably enriched at the bottom region of the cell. This enrichment was stronger than at the upper region of the cell, where the cleavage furrow was progressing (Fig. 3 B_9).

The late cleavage stage depicted in Fig. 4 *A* is distinguished from the previous stages by the accumulation of myosin II at the upper portion of the furrow. In the vertical midline section the area of strongest myosin II enrichment appeared V-shaped (Fig. 4 A_9), and in the cross section through the furrow it appeared as half of a ring that opened towards the bottom (Fig. 4 A_8). The distribution of myosin II in the final stage of Fig. 4 *B* is characterized by upright walls with the furrow forming a short tube between them (Fig. 4, B_6 and B_9). Myosin II was most prominently accumulated along the walls, whereas the tube region was not particularly enriched in myosin II (Fig. 4 B_9).

In none of the 68 stages of cytokinesis that were analyzed was myosin II found to be precisely enriched in the form of a closed ring at the site of the cleavage furrow. At early stages, the myosin tended to flank the furrow at both sides of the midline, and at later stages it associated with the steep walls bordering the furrow.

Phosphorylation-dependent Myosin II Redistribution in Compressed Cells

Neither in suspension nor on a surface did the cells display the ring of myosin II accumulation considered to be typical of mitotic cleavage in *Dictyostelium* cells. Therefore,

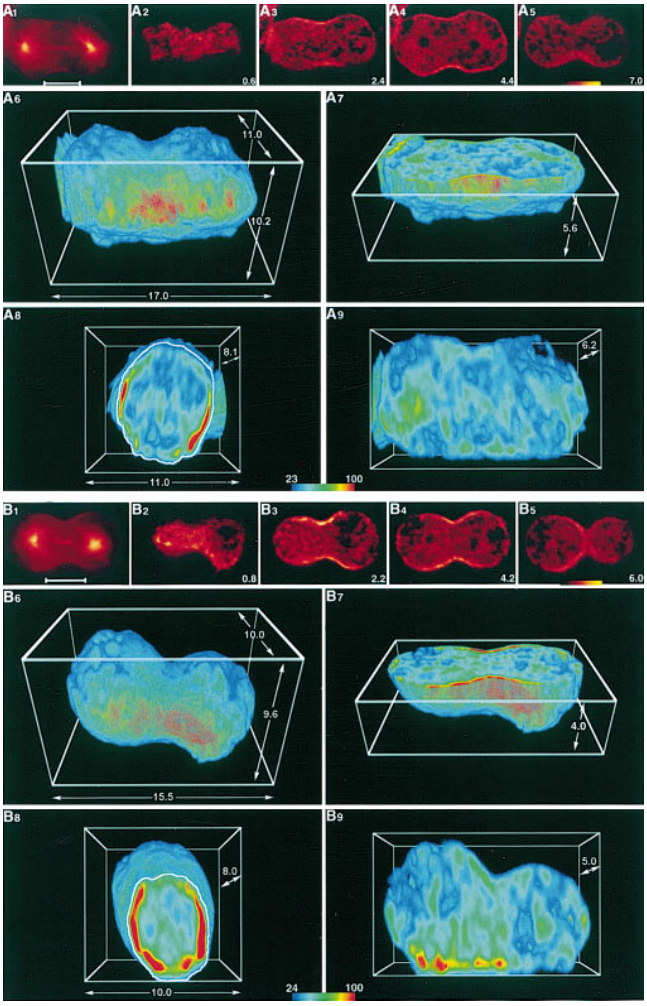

Figure 3. Myosin II distribution at two early stages of cytokinesis on a glass surface. Fixed cells were labeled with antibodies for myosin II and α-tubulin as for Fig. 1. The α-tubulin label shown in A_1 and B_1 visualizes the microtubule asters and elongated spindle diagnostic of mitotic cells in late anaphase or telophase. (A_2–A_5 and B_2–B_5) show the myosin II label in series of confocal sections from bottom to top of the cells. Numbers are distances in micrometers from the substrate surface. The color code is from dark red (low fluorescence intensity) to light yellow (high intensity), as indicated on the linear scales. For A_6–A_9 and B_6–B_9, three-dimensional distributions of myosin II were derived from serial confocal sections. In A_6 and B_6, the cells are depicted as unopened, and only myosin II located in the cortical region of the cells is visualized, similar to Fig. 1. In A_7 and B_7, the cells are shown unroofed by a sagittal section, A_8 and B_8 are cross sections through the center of the cleavage furrow, and A_9 and B_9 are frontal sections through the midline of these cells. The boundaries of cross sections through the cleavage furrow are marked by a white outline. Fluorescence intensities in the sections are color-coded from dark blue to red as marked on the linear scales. Numbers at the left end of the scales indicate the extracellular background values represented in black. Intensity values >100 were only exceptionally obtained, and the red color at the right end of the bars was attributed to these voxels. For details of ray tracing and color coding, see Materials and Methods. Dimensions are given on the coordinates in micrometers. Bars, 5 μm.

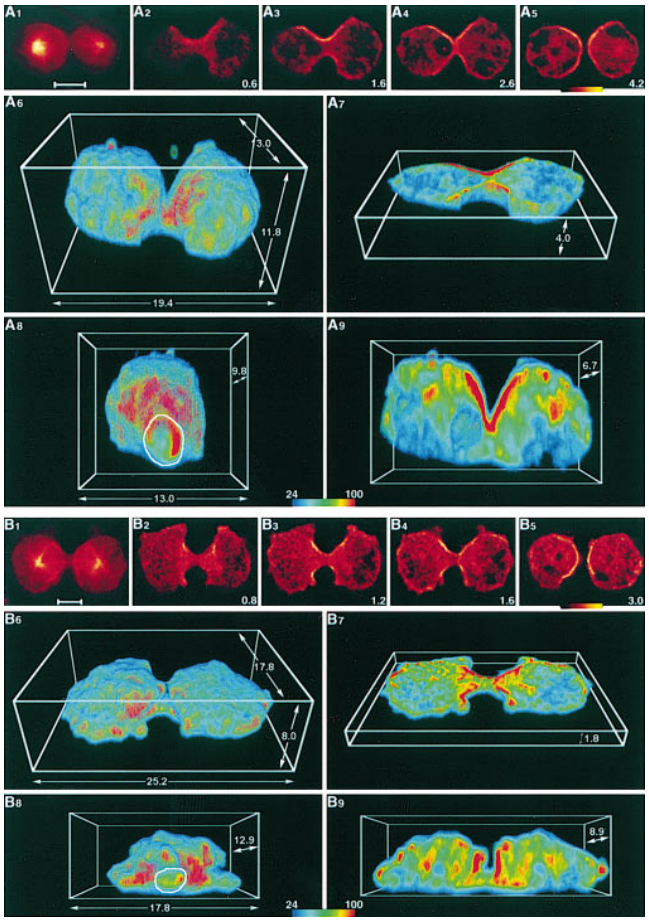

Figure 4. Myosin II distribution at two late stages of cytokinesis on a glass surface. This figure is organized in the same way as Fig. 3. A_1 and B_1 show labeled α-tubulin, A_2–A_5 and B_2–B_5 show myosin II label in four confocal sections from bottom to top of the cells. In A_6–A_9 and B_6–B_9, the distribution of myosin II is three-dimensionally reconstructed and visualized from the outside of the cells (A_6 and B_6) or with the cells optically sectioned in a sagittal plane (A_7 and B_7), through the cleavage furrow (A_8 and B_8), or frontally through their midline (A_9 and B_9). Bars, 5 μm.

we flattened the cells by compressing them between an agar layer and a glass coverslip to reproduce the conditions that had previously been used to study cytokinesis (Yumura et al., 1984). In response to a forced deformation, myosin II was profoundly redistributed in interphase as well as in mitotic cells. In the interphase stage, myosin II was translocated within minutes of compression into one or several crescent-shaped areas close to the cell surface (Fig. 5 *A*). In compressed mitotic cells, myosin II was translocated towards the cleavage furrow. At 6 min of compression, myosin II was strongly accumulated at the flanks of the furrow (Fig. 5 *B*). Within 15 min of compression, this distribution changed into a strict concentration of myosin II in the middle of the furrow. Only a negligible fraction of myosin II remained in the cytoplasmic space or in the cell cortex outside of that region. This distribution of myosin II is consistent with that previously observed under the same agar-overlay conditions (Kitanishi-Yumura and Fukui, 1989; Fukui and Inoué, 1991).

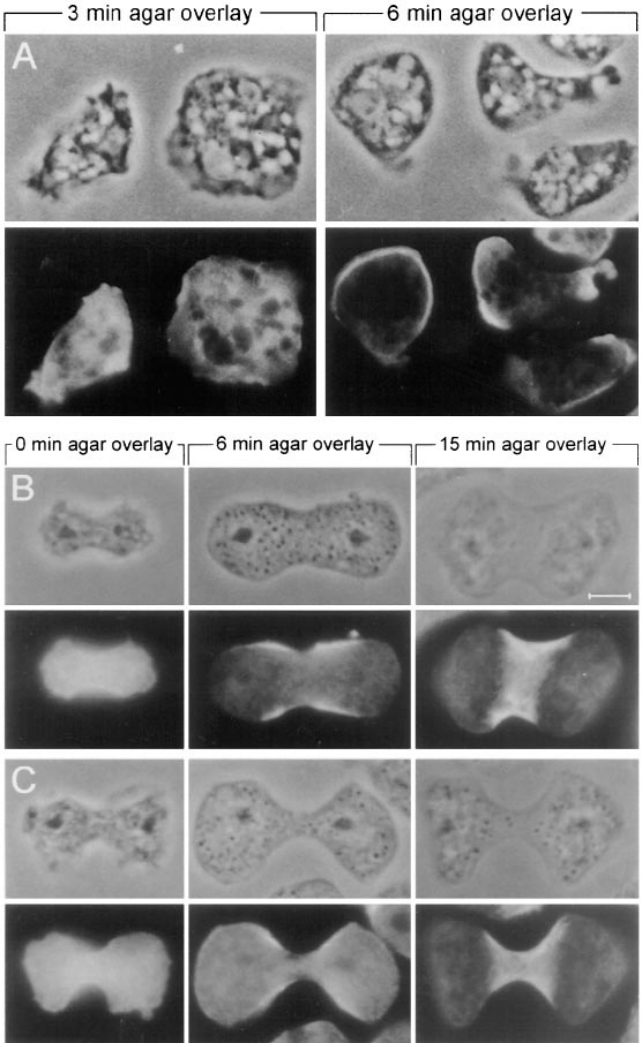

Figure 5. Mechanical stress–induced translocation of myosin II in interphase (*A*) and during mitosis (*B* and *C*). In *A*, interphase cells were fixed at short intervals after compression to demonstrate redistribution of myosin II in the flattened cells, thereby excluding influences of optical conditions that vary between uncompressed or compressed cells. For *B* and *C*, cells attached to a glass surface were incubated under a layer of fluid (*left*) as for Figs. 3 and 4 or were compressed under an agar layer for 6 min (*middle*) or 15 min (*right*). After these treatments, cells were fixed and antibody labeled for myosin II. Interphase cells (*A*) and examples of early (*B*) and late (*C*) stages of cytokinesis are shown in phase contrast (*upper panels*) and immunofluorescence images (*lower panels*). Bar, 5 μm.

The strong accumulation of myosin II at cortical areas of compressed interphase cells resembled the previously reported cortical location of "triple ala" myosin (Egelhoff et al., 1993; Gerisch et al., 1993). This myosin contains mutated heavy chains whose three phosphorylatable threonine residues were converted into alanine. Because of this similarity, we also subjected cells producing triple-ala myosin II to agar overlay conditions. No striking change in the distribution of this mutated myosin was found. Even before compression, the triple-ala myosin strongly accumulated at regions of the cell cortex (Fig. 6, *A* and *B*). The angular shape of the mutant cells contrasted with the rounded shape of wild-type cells, suggesting that the mutated myosin conferred a higher bending stiffness to the cell cortex. From these data we infer that mechanical stress elicits a gross translocation of myosin II from the cytoplasm to the cell cortex, and the difference between uncompressed and compressed cells is based on the regulation of heavy chain phosphorylation.

The picric acid/formaldehyde fixation procedure used in our experiments appropriately preserves cell shape, myosin and actin distribution, and reactivity with antibody or phalloidin. We obtained comparable results by the use of a fixation technique previously applied to the localization of myosin II in *Dictyostelium* (Egelhoff et al., 1991). The effect of compression was equally seen with this method (Fig. 6 *B*).

Three-dimensional Myosin II Patterns in Compressed Cells Undergoing Cytokinesis

To visualize the three-dimensional pattern of myosin II in compressed cells at an early stage and after completion of its translocation to the furrow upon mechanical stress, cells that divided under agar-overlay conditions were fixed, labeled with antibodies, and subjected to confocal microscopy in the same way as the uncompressed cells shown in Figs. 3 and 4. In Fig. 7, *A* and *B*, two cells at an early stage of cleavage are compared. One of these cells had been compressed for 6 min, the other for 15 min. In the cell fixed after 6 min (Fig. 7 *A*), myosin II accumulated mainly in zones that flanked the furrow. At one side of this particular cell, the myosin had already clustered in the furrow, as seen on top of the confocal sections of Fig. 7, A_2–A_5, and in the three-dimensional image of A_7. Myosin II accumulation was somewhat patchy in this cell, which suggests this represents an intermediate state in the translocation. At the final state of redistribution, attained after 15 min of compression (Fig. 7 *B*), myosin II had formed a flattened circular band in the furrow. The highest concentration of myosin II was found at both sides of the cell where the membrane had been most excessively bent between the glass and agar surfaces, as indicated by the red areas in B_8.

At later stages of cleavage furrow formation (Fig. 7, *C* and *D*), the redistribution of myosin II caused by compressing the cells appeared to be even more accentuated than at the earlier stages of Fig. 7, *A* and *B*. The cell shown in Fig. 7 *C* again represents an intermediate state at 6 min of compression. On one side of this cell, myosin II had clearly accumulated in regions that flanked the furrow, while on the other side it concentrated directly in the furrow. Fig. 7 *D* shows a cell in a corresponding stage of cleavage after 15 min of compression. Myosin II formed a solid plate in the center of this cell, rather than a ring in the cortical region of the furrow. The speckled appearance of the myosin II immunolabel seen in D_1–D_5 was most likely due to the formation of large myosin filaments, as reported previously for interphase cells treated in a similar manner (Yumura and Fukui, 1985).

Distribution of F-Actin in Dividing Cells

In parallel to the extensive redistribution of myosin II in compressed cells, we studied the pattern of filamentous ac-

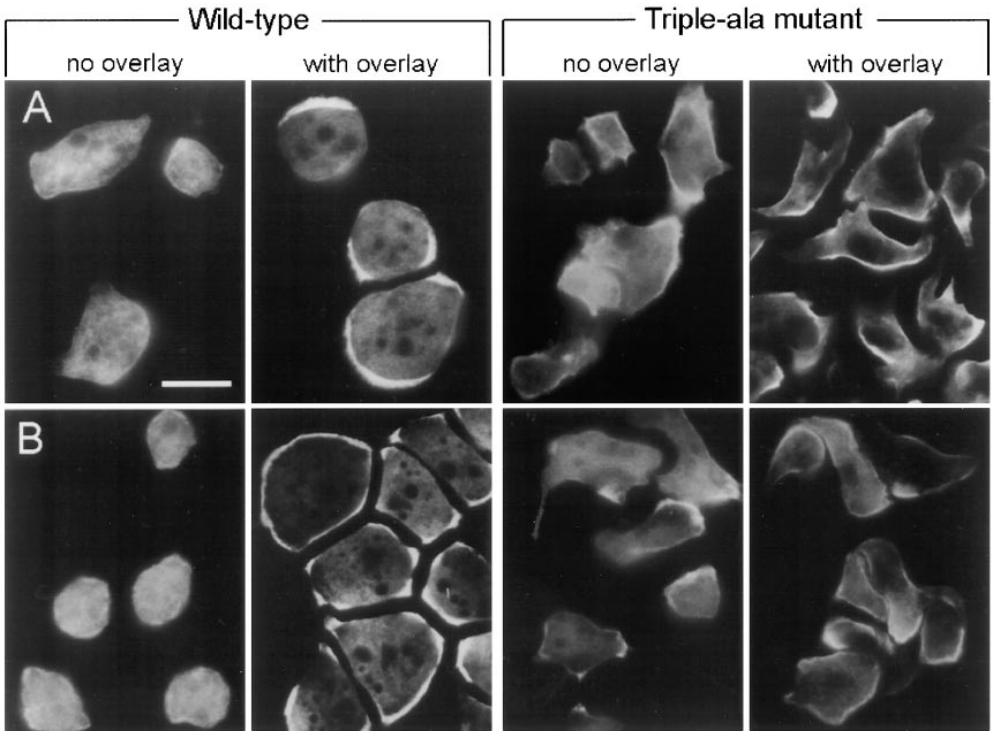

Figure 6. Phosphorylation dependence of the mechanical stress–induced translocation of myosin II. Wild-type AX2 cells (*left*) are compared with cells producing myosin II heavy chains in which three phosphorylatable threonine residues are replaced by alanine (*right*). For both strains, interphase cells are shown either uncompressed or compressed for 15 min by an agar overlay. The cells were either fixed by the picric acid/formaldehyde standard procedure used in the present paper (*A*) or in cold formaldehyde-acetone (*B*) (Egelhoff et al., 1991). The fixed cells were labeled with anti–myosin II antibody and viewed by conventional fluorescence microscopy. Bar, 10 μm.

tin. The phalloidin-labeled cell of Fig. 8 *A* exemplifies the F-actin pattern consistently obtained in the absence of mechanical pressure: F-actin formed a continuous cortical layer in the cleavage furrow as well as along other portions of the cell boundary and was conspicuously enriched in surface extensions at the poles of the cell or in patches close to the substrate. Only a slight enrichment of actin was observed in the cleavage furrow.

Fig. 8 *B* shows a phalloidin-labeled cell at post-telophase, which had been compressed for 15 min before fixation. As in the uncompressed cell of Fig. 8 *A*, F-actin was distributed throughout the cortical region of this cell and locally enriched in the form of patches. No accentuated accumulation in the cleavage furrow was recognizable.

Myosin II and Actin Dynamics Monitored by GFP Fusion Proteins

Static images of fixed cells, such as described in previous sections, can only show the distribution of myosin II and actin at a given moment in the cleavage process. To reveal the dynamics of assembly of these proteins during mitosis, GFP-tagged myosin II and actin were monitored in cells dividing under mechanical pressure. Before the onset of cleavage furrow formation, myosin II was found in an essentially uniform layer beneath the cell surface and was subsequently almost quantitatively transported to the incipient furrow (Fig. 9 *A*).

Two examples of the dynamics of actin assembly during cytokinesis are given in Fig. 9, *B* and *C*. In the first sequence, cleavage was initiated with no significant enrichment of GFP–actin in the furrow (Fig. 9 *B*). Later in the course of cytokinesis, actin delineated the furrow region and finally formed a patch in each of the daughter cells at the site of their disconnection.

The second GFP–actin sequence starts early before the onset of cleavage and shows a rotation of the spindle by 180° during anaphase and early telophase (Fig. 9 *C*, *top row*). Actin patches of irregular shape and size changed their position within the cell during this stage, but little accumulation of actin was recognizable at the cell border. The most obvious change in the distribution of actin during formation of the cleavage furrow was its strong recruitment to the highly dynamic protrusions that formed at the polar regions of the dividing cell (Fig. 9 *C*, *second row*). These protrusions reflected the varying directions of movement of the bodies of the incipient daughter cells, either away from each other or in a more lateral direction (Fig. 9 *C*, *third row*). GFP–actin proved to be only transiently accumulated in the cleavage furrow. Most of the actin in the furrow was derived from the patches that had been formed before the onset of cleavage and was therefore incorporated into the furrow in an asymmetrical fashion (14–16 min frames of Fig. 9 *C*).

The two cases shown in Fig. 9 illustrate the strongest accumulation of GFP–actin in the cleavage furrow that we have observed. Other cells formed a furrow with less distinct or even no obvious accumulation of actin. The intense enrichment of GFP–actin in the polar extensions of these cells was, however, always evident.

Discussion

Myosin II and Actin Localization in Cells Dividing in the Absence of Mechanical Stress

The results presented in this paper show that in cells dividing either in suspension or attached to a solid substrate under a layer of fluid, myosin II is not as strictly localized to

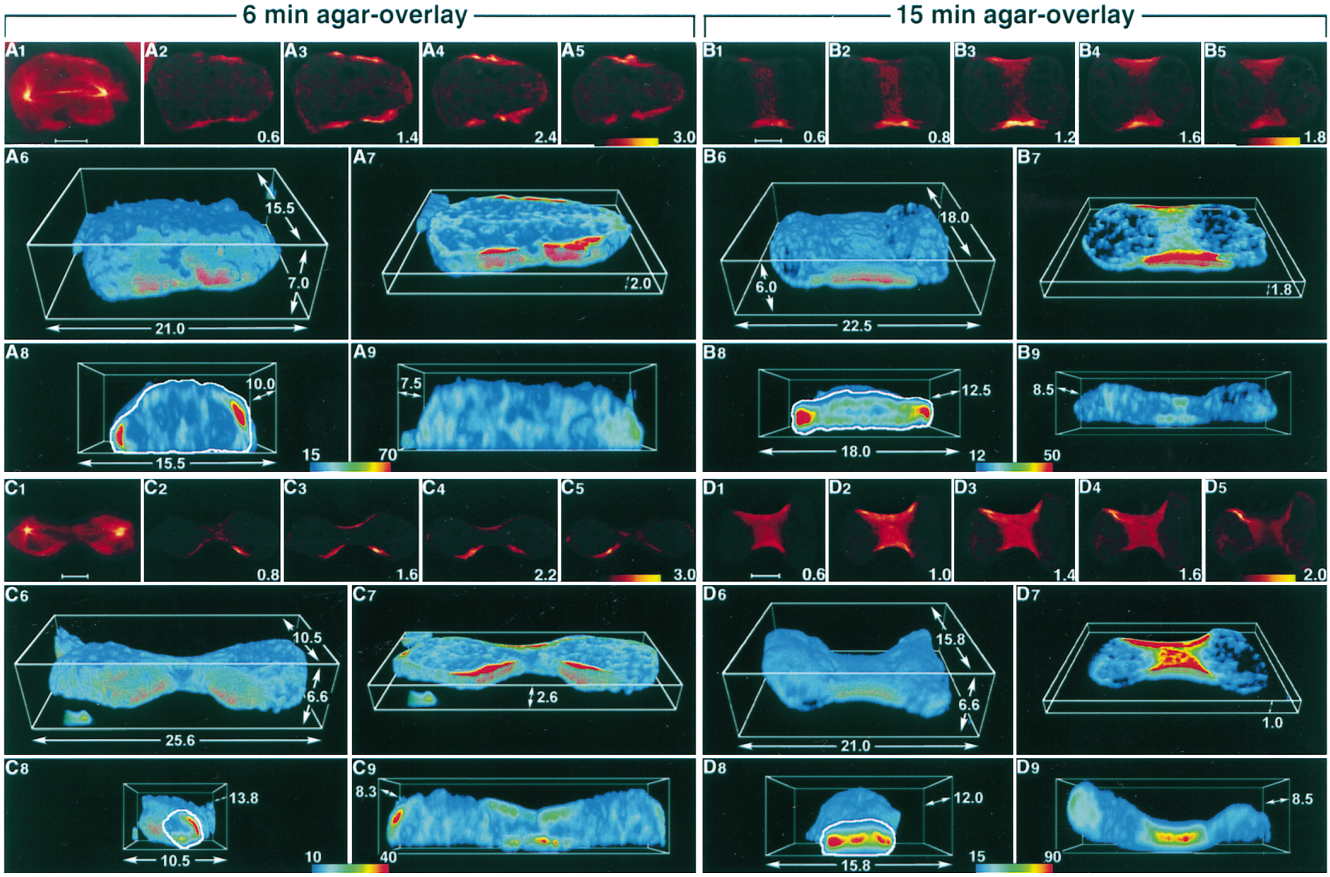

Figure 7. Myosin II distribution at early (*A* and *B*) and late (*C* and *D*) stages of cytokinesis in compressed cells. Before fixation, the cells had been compressed by agar overlay for either 6 min (*A* and *C*) or 15 min (*B* and *D*). *A1* and *C1* show microtubule labeling to indicate the stage of cytokinesis. In A_2–A_5 and C_2–C_5, and B_1–B_5 and D_1–D_5, myosin II label is shown in series of confocal sections. Numbers in these panels indicate distances in micrometers from the substrate surface. The three-dimensional myosin II distributions in *6–9* are reconstructed in a way comparable to those of the uncompressed cells shown in Figs. 3 and 4. Bars, 5 μm for *1–5*. In the other panels, dimensions are given in micrometers on the coordinates.

the cleavage furrow, as has been previously reported for *Dictyostelium* cells compressed between a glass and an agar surface (Fukui and Inoué, 1991). In fact, when no mechanical stress is applied, myosin II is primarily localized to regions of the cell cortex that flank the furrow towards the poles of the dividing cell, rather than to the center of the furrow (Figs. 3 to 4). Under the same conditions, F-actin is seen to assemble in a continuous layer beneath the plasma membrane in a dividing cell, sometimes forming irregular patches (Fig. 8 *A*). Only in protrusions of the cells, which are extended from their polar regions during the late telophase and post-telophase, is F-actin consistently enriched. It is hard to imagine from these distributions of myosin II and actin that a contractile ring is formed by the coassembly of these proteins.

These results obtained in *Dictyostelium* are consistent with the conclusions drawn from detailed analyses of the orientation of myosin II and actin filaments in mammalian cells. The orientation of actin filaments in the cleavage furrow of rat kidney cells shows a complicated pattern (Fishkind and Wang, 1993). It is only on the portion of the surface that adheres to the substrate, which shows little or no cleavage activity, where microfilaments are seen to form large bundles along the equator. On the dorsal surface, where the furrow proceeds, the filaments remain essentially disoriented. A comprehensive study on the distribution of myosin II and the orientation of its filaments in dividing 3T3 fibroblasts led to the conclusion that fibers span the volume of the furrow region in three dimensions during ana- and telophase (DeBiasio et al., 1996). In an earlier study on dividing chicken embryo cells, Nunnally et al. (1980) reported that myosin II was concentrated in the furrow in only 37% of the cells.

Based on the distributions of myosin II and actin observed in dividing *Dictyostelium* cells, two questions are raised: (*a*) Does myosin II play a role in cytokinesis of these cells different from its proposed involvement in the formation of a contractile ring? (*b*) How is myosin II redistributed upon the deformation of cells that are squeezed between two surfaces?

Role of Myosin II as Compared with Other Proteins in Cytokinesis

Our finding that myosin II is normally enriched in the regions surrounding the cleavage furrow in *Dictyostelium* cells is consistent with the previous notion that myosin II, although not strictly required for cytokinesis, has a sup-

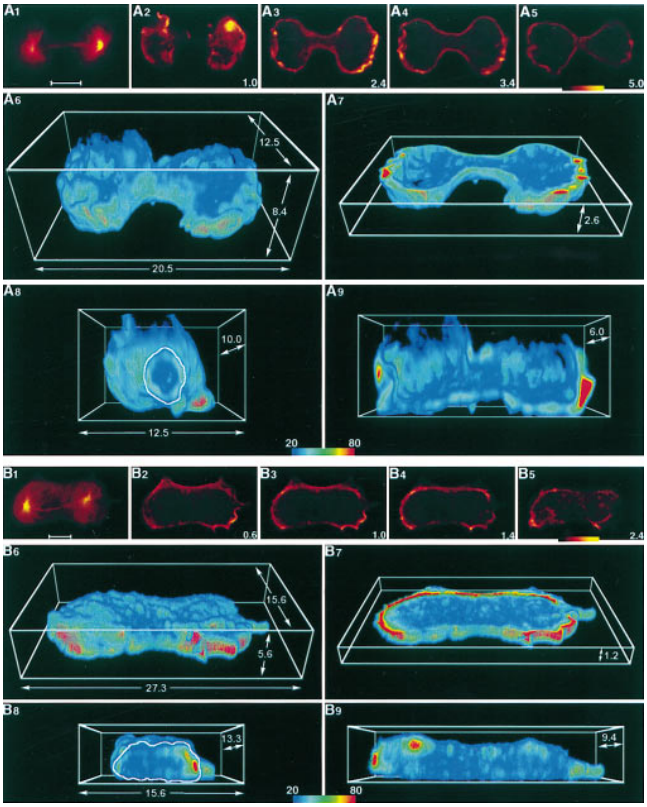

Figure 8. Distribution of F-actin in cells dividing in a fluid layer on a glass surface (*A*) or under an agar overlay (*B*). The microtubule antibody label in *A1* and the GFP–tubulin label in *B1* indicate the cells were in telophase. A_2–A_5 and B_2–B_5 show TRITC-phalloidin labeling in a series of confocal sections. Distances from the substrate are indicated in micrometers. Three-dimensional distributions of F-actin are shown in *6–9*. These images are constructed in parallel to those of Figs. 3 and 4, which show the distribution of myosin II. In the uncompressed cell (*A*) as well as the compressed one (*B*) F-actin is most strongly enriched in polar regions. Bars, 5 μm for *1–5*. In the other panels, dimensions are given on the coordinates in micrometers.

porting function in stabilizing the symmetry of cell shape during cytokinesis (Neujahr et al., 1997). In this manner, myosin II helps to keep the cleavage furrow in its correct position. Cells lacking myosin II need, on the average, a longer time to divide, and about 10% of them fail to complete cytokinesis, usually because of an imbalance in the hydrostatic pressure of the daughter cells. In these cases, cytoplasm streams through the furrow in one direction. If a nucleus is carried within the stream before the daughter cells separate, one of the daughter cells is resorbed by the other (Neujahr et al., 1997).

The fact that myosin II is not essential for cytokinesis in *Dictyostelium* cells attached to a substrate implies that all of the components indispensable for the formation of a cleavage furrow are still present in myosin II–null cells. In *Dictyostelium* cells, as in the blastulae of sea urchins (Rappaport, 1961), the position of a furrow is specified primarily by the asters of microtubules at the poles of the mitotic apparatus (Neujahr et al., 1997; Niewöhner et al., 1997). The mitotic spindle is dispensable in these cells as far as specification of a furrow in the cell cortex is concerned.

The question is then which proteins in the cell cortex respond to the signals from the asters in defining the position of the furrow and which are required to bring about the changes in cell shape that lead to separation of the daughter cells. Candidate proteins have been identified in *Dictyostelium* by mutagenesis. The proteins of interest can be classified in signal transduction elements that might exchange signals between the microtubule and actin systems, and in components of the cell cortex that determine either the viscoelastic properties of the actin network or the coupling of actin filaments to the plasma membrane. GTPases of the rac family are known to be involved in cytokinetic signaling. Elimination of rac E (Larochelle et al., 1996), overexpression of DGAP1, a homologue of GTPase activating proteins, or elimination of a related protein in *Dictyostelium* causes defects in cytokinesis (Faix and Dittrich, 1996; Adachi et al., 1997). A pronounced impairment of mitotic cleavage has been obtained by eliminating the two isoforms of the actin-bundling protein, cortexillin (Faix et al., 1996). *Dictyostelium* talin is also involved in cytokinesis (Niewöhner et al., 1997). Cortexillins and talin play important roles in the maintenance of the bending stiffness of the cell cortex and in coupling the cortical actin layer to the plasma membrane (Simson et al., 1998). Coronin is another actin-associated protein whose absence leads to an impairment of cytokinesis (DeHostos et al., 1993). This is of particular interest since coronin is exclusively enriched in the dynamic extensions formed at the poles of a dividing cell, indicating that activities in the furrow and polar regions contribute to the separation of daughter cells (DeHostos et al., 1993; Neujahr et al., 1997).

The data emphasizing the importance of proteins other than myosin II in cytokinesis provide a framework for reconsidering the mechanics of mitotic cleavage with the aim to complement, modify, or replace the contractile ring hypothesis of cleavage furrow formation. The finding that *Dictyostelium* cells need myosin II for cytokinesis only under certain conditions may also apply to other cells. The mechanical conditions of blastomere formation in early embryogenesis seem to resemble those of *Dictyostelium* cells in suspension, where myosin II is required. In sea urchin eggs, for instance, blastomeres undergo massive changes in shape while being attached only to their neighbors, which are not rigid and moreover change their own shape as they divide (for an overview see Rappaport, 1986). By the same argument, myosin II activities might be more critical for the anchorage-independent division of tumor cells than for cells attached to an extracellular matrix, on which they can apply traction (Burton and Taylor, 1997).

Significance of Mechanical Stress–induced Myosin II Translocation

Mechanical stress is one of several conditions that can alter the distribution of myosin II in *Dictyostelium* cells. ATP depletion leads to the clustering of myosin II together with actin filaments in the central portion of the cells, probably in the form of rigor complexes. These complexes are immediately dispersed upon recovery of ATP synthesis (Jungbluth et al., 1994). Hyperosmotic stress causes myosin II to form a shell around the shrunken cells

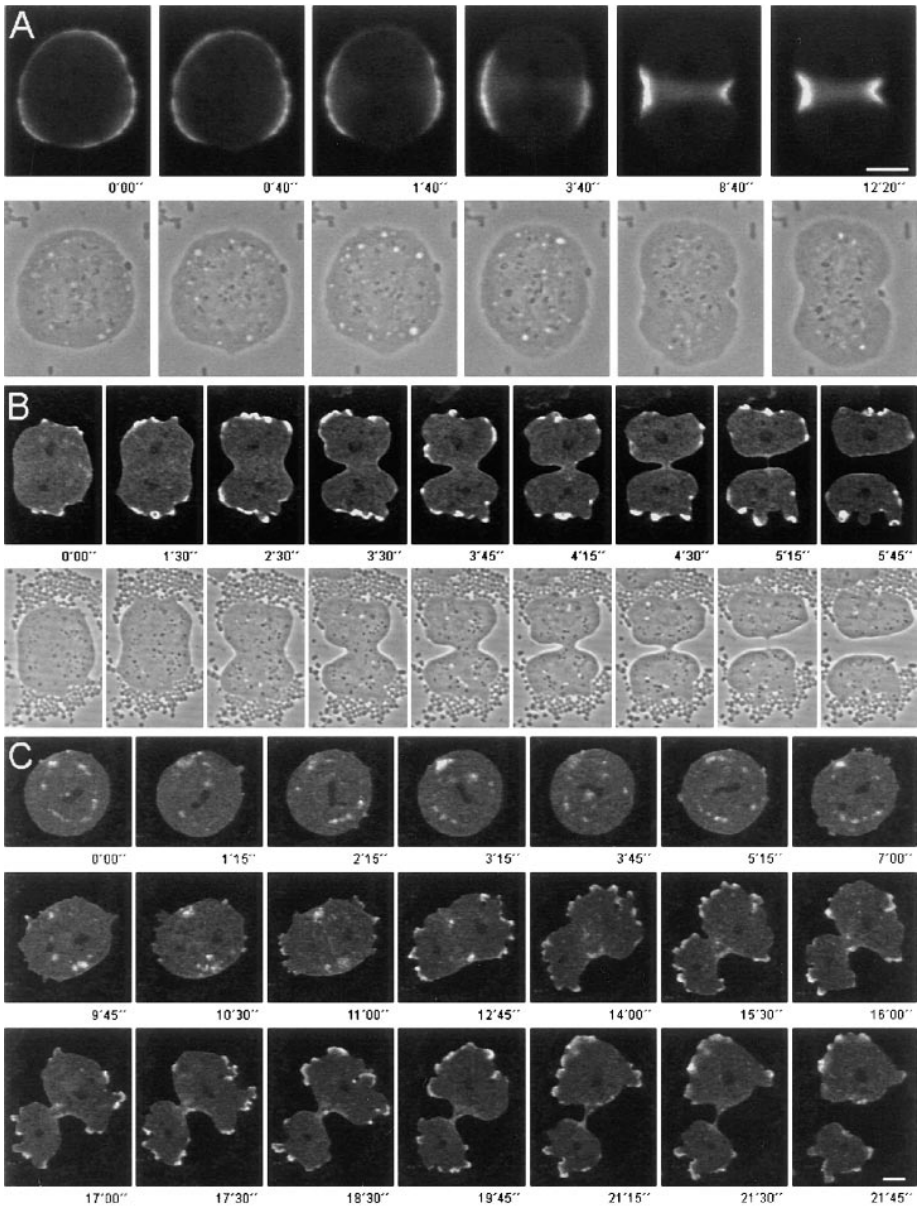

Figure 9. Myosin II (*A*) and actin (*B* and *C*) dynamics visualized by GFP fusion proteins during cytokinesis of cells compressed by agar overlay. The time series of *A* reveals translocation of cortical myosin II into the cleavage furrow. The series of *B* and *C* exemplify changes in the distribution of GFP–actin in two cells dividing under an agar overlay. Fluorescence intensities were recorded in the confocal mode. For the cells shown in *A* and *B*, fluorescence images (*top*) are shown in parallel with phase-contrast images (*bottom*). To avoid sensitization by fluorescent compounds taken up from nutrient medium, cells were cultivated on bacteria. On the bottom of each frame, times after beginning of the record are given in minutes and seconds. Bars, 5 μm.

and causes actin to accumulate separately in protrusions at the outer surface of this shell (Kuwayama et al., 1996). The translocation of myosin II in mechanically compressed cells, where actin accumulates at the fronts of the commencing daughter cells and myosin II in the cleavage furrow, differs from both these types of re-distribution.

Although excessive recruitment of myosin II to the cleavage furrow is not essential for a mitotic *Dictyostelium* cell to divide, it might have a more conspicuous function under the aggravating conditions of mechanical stress. Division is retarded in compressed wild-type cells (Figs. 9 vs. Fig. 2), and myosin II–null cells have even more severe problems dividing under an agar overlay (Neujahr, R., unpublished results). In interphase cells, myosin II accumulates in cell projections that are being retracted (Moores et al., 1996) and reinforces retraction of the tail of a cell (Jay et al., 1995). Under the natural conditions of life in soil, myosin II may reinforce separation of the daughter cells by retraction of their presumptive tails, which are derived from the cleavage furrow.

Relationship of Myosin II Translocation to Cell Surface Capping

Compression of interphase cells causes myosin II to accumulate in crescent-shaped areas that are considered to be the tail regions of the cells (Yumura and Fukui, 1985). Since in mitotic cells the cleavage furrow marks the tails of the incipient daughter cells, it is conceivable that compression of these cells would cause the myosin to accumulate in the furrow (Fig. 5). We hypothesize that this mechanical stress–induced redistribution of myosin II occurs in two steps, one probably accomplished by dephosphorylation of the myosin II heavy chains and the other by a process related to the capping of cell surface proteins. Translocation of myosin II from the cytoplasm to the cell cortex is caused

by the dephosphorylation of three threonine residues at its heavy chains (Lück-Vielmetter et al., 1990; Egelhoff et al., 1993; Gerisch et al., 1993), which favors the assembly of monomeric myosin II into bipolar filaments (Pasternak et al., 1989) and leads to cortical accumulation of the myosin in uncompressed cells almost indistinguishable from that in compressed cells (Fig. 6). Because of its strong accumulation in cortical regions of the cells, we assume that myosin II is arrested under mechanical stress in a threonine-dephosphorylated state. Mechanical stress might inhibit a myosin II heavy chain kinase (Abuelneel et al., 1996) or activate a phosphatase (Kuczmarski and Pagone, 1986). It is comprehensible in this context that the conversion of the three phosphorylatable threonine residues into alanine does not prevent the myosin from its accumulation in the cleavage furrow (Yumura and Uyeda, 1997).

Dephosphorylation of the myosin II heavy chains causes assembly of myosin II in the cell cortex but does not explain its translocation to the tail of the cells (Gerisch et al., 1993) or to the cleavage furrow (Fig. 5). Therefore, a second step of mechanical stress–induced myosin II redistribution is proposed, which by three arguments is comparable to the capping of cell surface proteins in response to their cross-linkage by antibodies or lectins. (*a*) Particle attachment is considered to have a stronger cross-linking effect than a soluble lectin (Jay and Elson, 1992). Therefore, the compression of cells between two surfaces should mimic a very strong capping stimulus. (*b*) In myosin II–null mutants, the capping of concanavalin A–linked glycoproteins is impaired (Jay and Elson, 1992). On the contrary, it is enhanced in cells producing the mutated triple-alanine heavy chains (Ecke, M., and G. Gerisch, unpublished results), suggesting that cross-linked membrane proteins couple to cortical myosin II in its threonine-dephosphorylated state. (*c*) When cell surface capping is induced by concanavalin A in cells compressed by an agar overlay, the capped cell-surface material localizes on top of the crescents of myosin II (Gerisch, G., and M. Ecke, manuscript in preparation). This result establishes a direct relationship between cell surface capping and myosin II redistribution. It suggests that in *Dictyostelium* cells myosin II comigrates beneath the membranes with cross-linked glycoproteins on the cell surface, as it does in fact in *Entamoeba histolytica* (Arhets et al., 1995). For *Dictyostelium* cells, one only needs to assume that compression is necessary to inhibit disassembly and thus retain the sequestered myosin II at the tail of the cells or, during mitosis, at the cleavage furrow.

We thank our colleagues from the Max-Planck-Institut (MPI) für Biochemie, Martinsried, Germany: John Murphy for the scanning electron micrographs, Alicja Baskaya for the monoclonal antibody, Jana Köhler for cooperation in fluorescence scanning, Monika Westphal for the GFP–α-tubulin–producing cells, and Gerard Marriott and Chris Clougherty for critically reading the manuscript. The GFP-myosin–producing cells were a gift from Sheri L. Moores and James H. Sabry (Stanford University, Stanford, CA). The triple-ala mutant was constructed by Dorothea Lück-Vielmetter (MPI für Biochemie) in cooperation with James A. Spudich and Thomas T. Egelhoff (Stanford University).

The work was supported by grants of the Deutsche Forschungsgemeinschaft (SFB 266/D7) and the Fonds der Chemischen Industrie to G. Gerisch.

Received for publication 30 July 1997 and in revised form 31 October 1997.

References

Abuelneel, K., M. Karchi, and S. Ravid. 1996. *Dictyostelium* myosin II is regulated during chemotaxis by a novel protein kinase C. *J. Biol. Chem*. 271:977–984.

Adachi, H., Y. Takahashi, T. Hasebe, M. Shirouzu, S. Yokoyama, and K. Sutoh. 1997. *Dictyostelium* IQGAP-related protein specifically involved in the completion of cytokinesis. *J. Cell Biol.* 137:891–898.

Arhets, P., P. Gounon, P. Sansonetti, and N. Guillen. 1995. Myosin II is involved in capping and uroid formation in the human pathogen *Entamoeba hystolytica. Infect. Immun.* 63:4358–4367.

Burton, K., and D.L. Taylor. 1997. Traction forces of cytokinesis measured with optically modified elastic substrata. *Nature.* 385:450–454.

Cao, L.-G., and Y.-L. Wang. 1990*a*. Mechanism of the formation of contractile ring in dividing cultured animal cells. I. Recruitment of preexisting actin filaments into the cleavage furrow. *J. Cell Biol.* 110:1089–1095.

Cao, L.-G., and Y.-L. Wang. 1990*b*. Mechanism of the formation of contractile ring in dividing cultured animal cells. II. Cortical movement of microinjected actin filaments. *J. Cell Biol.* 111:1905–1911.

Claviez, M., M. Brink, and G. Gerisch. 1986. Cytoskeletons from a mutant of *Dictyostelium discoideum* with flattened cells. *J. Cell Sci.* 86:69–82.

DeBiasio, R.L., G.M. LaRocca, P.L. Post, and D.L. Taylor. 1996. Myosin II transport, organization, and phosphorylation: evidence for cortical flow/solation-contraction coupling during cytokinesis and cell locomotion. *Mol. Biol. Cell.* 7:1259–1282.

DeHostos, E.L., C. Rehfueß, B. Bradtke, D.R. Wadell, R. Albrecht, J. Murphy, and G. Gerisch. 1993. *Dictyostelium* mutants lacking the cytoskeletal protein coronin are defective in cytokinesis and cell motility. *J. Cell Biol.* 120:163–173.

DeLozanne, A., and J.A. Spudich. 1987. Disruption of the *Dictyostelium* myosin heavy chain gene by homologous recombination. *Science*. 236:1086–1091.

Egelhoff, T.T., S.S. Brown, and J.A. Spudich. 1991. Spatial and temporal control of nonmuscle myosin localization: identification of a domain that is necessary for myosin filament disassembly in vivo. *J. Cell Biol.* 112:677–688.

Egelhoff, T.T., R.J. Lee, and J.A. Spudich. 1993. *Dictyostelium* myosin heavy chain phosphorylation sites regulate myosin filament assembly and localization in vivo. *Cell.* 75:363–371.

Faix, J., and W. Dittrich. 1996. DGAP1, a homologue of rasGTPase activating proteins that controls growth, cytokinesis, and development in *Dictyostelium discoideum*. *FEBS Lett.* 394:251–257.

Faix, J., M. Steinmetz, H. Boves, R.A. Kammerer, F. Lottspeich, U. Mintert, J. Murphy, A. Stock, U. Aebi, and G. Gerisch. 1996. Cortexillins, major determinants of cell shape and size, are actin-bundling proteins with a parallel coiled-coil tail. *Cell.* 86:631–642.

Fishkind, D.J., and Y.-L. Wang. 1993. Orientation and three-dimensional organization of actin filaments in dividing cultured cells. *J. Cell Biol.* 123:837–848.

Fishkind, D.J., and Y.-L. Wang. 1995. New horizons for cytokinesis. *Curr. Biol.* 7:23–31.

Fukui, Y., T.J. Lynch, H. Brzeska, and E.D. Korn. 1989. Myosin I is located at the leading edges of locomoting *Dictyostelium* amoebae. *Nature*. 341:328–331.

Fukui, Y., and S. Inoué. 1991. Cell division in *Dictyostelium* with special emphasis on actomyosin organization in cytokinesis. *Cell Motil. Cytoskel.* 18:41–54.

Gerisch, G., R. Albrecht, E. De Hostos, E. Wallraff, C. Heizer, M. Kreitmeier, and A. Müller-Taubenberger. 1993. Actin-associated proteins in motility and chemotaxis of *Dictyostelium* cells. *In* The Society of Experimental Biology 1993, Symposium No. 47, Cell Behaviour: Adhesion and Motility. G. Jones, C. Wigley, and R. Warn, editors. The Company of Biologists Ltd., Cambridge, UK, CB2 3EJ. 297–315.

Hanakam, F., R. Albrecht, C. Eckerskorn, M. Matzner, and G. Gerisch. 1996. Myristoylated and non-myristoylated forms of the pH sensor protein hisactophilin II: intracellular shuttling to plasma membrane and nucleus monitored in real time by a fusion with green fluorescent protein. *EMBO (Eur. Mol. Biol. Organ.) J.* 15:2935–2943.

Humbel, P.K., and E. Biegelmann. 1992. A preparation protocol for postembedding immunoelectron microscopy of *Dictyostelium discoideum* cells with monoclonal antibodies. *Scan. Microsc.* 68:817–825.

Jay, P.Y., and E.L. Elson. 1992. Surface particle transport mechanism independent of myosin II in *Dictyostelium*. *Nature.* 356:438–440.

Jay, P.Y., P.A. Pham, S.A. Wong, and E.L. Elson. 1995. A mechanical function of myosin II in cell motility. *J. Cell Sci.* 108:387–393.

Jungbluth, A., V. von Arnim, E. Biegelmann, B. Humbel, A. Schweiger, and G. Gerisch. 1994. Strong increase in the tyrosine phosphorylation of actin upon inhibition of oxidative phosphorylation: correlation with reversible rearrangements in the actin skeleton of *Dictyostelium* cells. *J. Cell Sci.* 107:117–125.

Kilmartin, J.V., B. Wright, and C. Milstein. 1982. Rat monoclonal antitubulin antibodies derived by using a new nonsecreting rat cell line. *J. Cell Biol.* 93: 576–582.

Kitanishi-Yumura, T., and Y. Fukui. 1989. Actomyosin organization during cytokinesis: reversible translocation and differential redistribution in *Dictyostelium*. *Cell Motil. Cytoskel.* 12:78–89.

Knecht, D.A., and W.F. Loomis. 1987. Antisense RNA inactivation of myosin heavy chain gene expression in *Dictyostelium discoideum*. *Science*. 236:1081–1086.

Kuczmarski, E.R., and J. Pagone. 1986. Myosin specific phosphatases isolated from *Dictyostelium discoideum. J. Musc. Res. Cell Motil.* 7:510–516.

Kuwayama, H., M. Ecke, G. Gerisch, and P.J.M. Van Haastert. 1996. Protection against osmotic stress by cGMP-mediated myosin phosphorylation. *Science*. 271:207–209.

Larochelle, D.A., K.K. Vithalani, and A. DeLozanne. 1996. A novel member of the *rho* family of small GTP-binding proteins is specifically required for cytokinesis. *J. Cell Biol.* 133:1321–1329.

Levoy, M. 1988. Display of surfaces from volume data. *In* Volume Visualization. A. Kaufman, editor. IEEE Computer Soc. Press, Los Alamos, CA. 135–143.

Lück-Vielmetter, D. 1992. Molekulargenetische Untersuchungen zur Rolle von Myosin II bei der Chemotaxis. Ph.D. thesis. Ludwig-Maximiliaus Universität München, München, Germany. 133 pp.

Lück-Vielmetter, D., M. Schleicher, B. Grabatin, J. Wippler, and G. Gerisch. 1990. Replacement of threonine residues by serine and alanine in a phosphorylatable heavy chain fragment of *Dictyostelium* myosin II. *FEBS Lett.* 269: 239–243.

Mabuchi, I. 1994. Cleavage furrow: timing of emergence of contractile ring actin filaments and establishment of the contractile ring by filament bundling in sea urchin eggs. *J. Cell Sci.* 107:1853–1862.

Maupin, P., and T.D. Pollard. 1986. Arrangement of actin filaments and myosin-like filaments in the contractile ring and of actin-like filaments in the mitotic spindle of dividing HeLa cells. *J. Ultrastruct. Mol. Struct. Res.* 94:92–103.

Moores, S.L., J.H. Sabry, and J.A. Spudich. 1996. Myosin dynamics in live *Dictyostelium* cells. *Proc. Natl. Acad. Sci. USA*. 93:443–446.

Neujahr, R., C. Heizer, and G. Gerisch. 1997. Myosin II-independent processes in mitotic cells of *Dictyostelium discoideum*: redistribution of the nuclei, rearrangement of the actin system and formation of the cleavage furrow. *J. Cell Sci.* 110:123–137.

Niewöhner, J., I. Weber, M. Maniak, A. Müller-Taubenberger, and G. Gerisch. 1997. Talin-null cells of *Dictyostelium* are strongly defective in adhesion to particle and substrate surfaces and slightly impaired in cytokinesis. *J. Cell Biol.* 138:349–361.

Nunnally, M.H., J.M. D'Angelo, and S.W. Craig. 1980. Filamin concentration in cleavage furrow and midbody region: frequency of occurrence compared with that of α-actinin and myosin. *J. Cell Biol.* 87:219–226.

Opas, J., and M.S. Soltynska. 1978. Reorganization of the cortical layer during cytokinesis in mouse blastomeres. *Exp. Cell Res.* 113:208–211.

Otto, J.J., and T.E. Schroeder. 1990. Association of actin and myosin in the contractile ring. *Ann. NY Acad. Sci.* 582:179–184.

Pagh, K., and G. Gerisch. 1986. Monoclonal antibodies binding to the tail of *Dictyostelium discoideum* myosin: their effects on antiparallel and parallel assembly and actin-activated ATPase activity. *J. Cell Biol.* 103:1527–1538.

Pasternak, C., P.F. Flicker, S. Ravid, and J.A. Spudich. 1989. Intermolecular versus intramolecular interactions of *Dictyostelium* myosin: possible regulation by heavy chain phosphorylation. *J. Cell Biol.* 109:203–210.

Rappaport, R. 1961. Experiments concerning the cleavage stimulus in sand dollar eggs. *J. Exp. Zool.* 148:81–89.

Rappaport, R. 1986. Establishment of the mechanism of cytokinesis in animal cells. *Int. Rev. Cytol.* 105:245–281.

Satterwhite, L.L., and T.D. Pollard. 1992. Cytokinesis. *Curr. Opin. Cell Biol.* 4: 43–52.

Schroeder, T.E. 1990. The contractile ring and furrowing in dividing cells. *Ann. NY Acad. Sci.* 582:78–87.

Simson, R., E. Wallraff, J. Faix, J. Niewöhner, G. Gerisch, and E. Sackmann. 1998. Membrane bending modulus and adhesion energy of wild-type and mutant cells of *Dictyostelium* lacking talin or cortexillins. *Biophys. J.* In press.

Sussman, M. 1966. Biochemical and genetic methods in the study of cellular slime mold development. *Methods Cell Physiol.* 2:397–410.

Weber, I., E. Wallraff, R. Albrecht, and G. Gerisch. 1995. Motility and substratum adhesion of *Dictyostelium* wild-type and cytoskeletal mutant cells: a study by RICM/bright-field double-view image analysis. *J. Cell Sci.* 108: 1519–1530.

Westphal, M., A. Jungbluth, M. Heidecker, B. Mühlbauer, C. Heizer, J.-M. Schwartz, G. Marriott, and G. Gerisch. 1997. Microfilament dynamics during cell movement and chemotaxis monitored using a GFP-actin fusion protein. *Curr. Biol.* 7:176–183.

Yonemura, S., and S. Kinoshita. 1986. Actin filament organization in the sand dollar egg cortex. *Dev. Biol.* 115:171–183.

Yumura, S., and Y. Fukui. 1985. Reversible cyclic AMP-dependent change in distribution of myosin thick filaments in *Dictyostelium*. *Nature*. 314:194–196.

Yumura, S., H. Mori, and Y. Fukui. 1984. Localization of actin and myosin for the study of ameboid movement in *Dictyostelium* using improved immunofluorescence. *J. Cell Biol.* 99:894–899.

Yumura, S., and T.Q.P. Uyeda. 1997. Myosin II can be localized to the cleavage furrow and to the posterior region of *Dictyostelium* amoebae without control by phosphorylation of myosin heavy and light chains. *Cell Motility Cytoskel.* 36:313–322.